THE JOURNAL OF BIOLOGICAL CHEMISTRY VOL. 286, NO. 26, pp. 23234–23246, July 1, 2011

Idas, a Novel Phylogenetically Conserved Geminin-related Protein, Binds to Geminin and Is Required for Cell Cycle Progression*[S]

Received for publication, December 2, 2010, and in revised form, April 30, 2011 Published, JBC Papers in Press, May 4, 2011, DOI 10.1074/jbc.M110.207688

Dafni-Eleutheria Pefani[‡], Maria Dimaki[‡], Magda Spella[§], Nickolas Karantzelis[§], Eirini Mitsiki[¶], Christina Kyrousi[§], Ioanna-Eleni Symeonidou[‡], Anastassis Perrakis[¶], Stavros Taraviras[§], and Zoi Lygerou[‡1]

From the [‡]Laboratory of Biology, School of Medicine, University of Patras, 26505 Rio, Patras, Greece, the [§]Laboratory of Physiology, School of Medicine, University of Patras, 26505 Rio, Patras, Greece, and the [¶]Division of Biochemistry, Netherlands Cancer Institute, Plesmanlaan 121, 1066CX Amsterdam, The Netherlands

Development and homeostasis of multicellular organisms relies on an intricate balance between cell proliferation and differentiation. Geminin regulates the cell cycle by directly binding and inhibiting the DNA replication licensing factor Cdt1. Geminin also interacts with transcriptional regulators of differentiation and chromatin remodelling factors, and its balanced interactions are implicated in proliferation-differentiation decisions during development. Here, we describe Idas (Idas being a cousin of the Gemini in Ancient Greek Mythology), a previously uncharacterised coiled-coil protein related to Geminin. We show that human Idas localizes to the nucleus, forms a complex with Geminin both in cells and *in vitro* through coiled-coil mediated interactions, and can change Geminin subcellular localization. Idas does not associate with Cdt1 and prevents Geminin from binding to Cdt1 *in vitro*. Idas depletion from cells affects cell cycle progression; cells accumulate in S phase and are unable to efficiently progress to mitosis. Idas protein levels decrease in anaphase, whereas its overexpression causes mitotic defects. During development, we show that Idas exhibits high level expression in the choroid plexus and the cortical hem of the mouse telencephalon. Our data highlight Idas as a novel Geminin binding partner, implicated in cell cycle progression, and a putative regulator of proliferation-differentiation decisions during development.

Development and homeostasis of multicellular organisms depends on the generation of the appropriate number of cells through cell proliferation and the acquisition of specialized cell functions through cell differentiation. Geminin has been suggested to regulate proliferation-differentiation decisions through balanced interactions with the DNA replication licensing factor Cdt1 and factors regulating transcription during development (1).

Geminin, initially identified as a substrate of the Anaphase Promoting Complex/Cyclosome (APC/C) ubiquitin ligase during mitosis (2), was shown to regulate DNA replication by directly binding to and inhibiting the DNA replication licensing factor Cdt1 (3–5). Geminin binding to Cdt1 during the S and G_2 phases of the cell cycle ensures that licensing of a further round of DNA replication is inhibited until the end of mitosis (6, 7). Geminin depletion causes over-replication, DNA damage, G_2/M arrest (8–11), and centrosome over-duplication (12) in a cell type-specific manner (13). Geminin overexpression in human cell lines is also cell type-specific, leading to arrest at the G_1/S phase transition or a defective S-phase followed by apoptosis (14).

Geminin was also identified as a putative regulator of differentiation, as its overexpression promoted the expansion of the neural plate in *Xenopus* embryos (15). Geminin was shown to interact with transcriptional regulators of differentiation, such as Six3 (16), Hox and Polycomb family members (17), the catalytic subunit of the SWI/SNF chromatin remodeling complex, Brg1/Brm (18), and regulators of Sox2 gene transcription (19), thereby modulating proliferation-differentiation decisions during development.

Geminin balanced interactions with its multiple binding partners are central to its function in the coordination of proliferation and differentiation. The central region of Geminin, containing the Geminin coiled-coil, is sufficient for interactions with Cdt1 and inhibition of licensing and mediates homodimerization of Geminin (20–23). In this study we introduce a previously uncharacterized human protein that is similar to Geminin in its central coiled-coil region. We name this protein Idas (Idas being a cousin of the Gemini in Ancient Greek Mythology). We show that Idas binds to the Geminin coiled-coil region and can modulate Geminin ability to bind Cdt1. Our data highlight Idas as a novel Geminin binding partner and regulator.

EXPERIMENTAL PROCEDURES

Bioinformatics Analysis—Tblastn (NCBI) was used to search expressed sequences from the human genome using the hGeminin protein sequence as query. mRNAs deriving from 5q11.2, on chromosome 5, were identified as encoding a protein with significant similarity to Geminin. This region is currently annotated as LOC345643. Gene2EST was used to identify

* This work was supported by the Association for International Cancer Research, European Grants HYGEIA and 3D-Repertoire, and Erasmus and FEBS Summer Fellowships (to D. P. and N. K.).

[S] The on-line version of this article (available at http://www.jbc.org) contains supplemental Figs. 1–4.

The nucleotide sequence(s) reported in this paper has been submitted to the GenBank™/EBI Data Bank with accession number(s) FR854393.

[1] To whom correspondence should be addressed. Tel.: 30-2610-997689; Fax: 30-2610-991769; E-mail: lygerou@med.upatras.gr.

Expressed Sequence Tags from this locus. The expression of LOC345643 is supported by 1 full-length cDNA (clone CS0DK002YL21) and 10 Expressed Sequence Tags that represent sequence reads from 5 cDNAs from HeLa cells (clone CS0DK002YL21), Jurkat cells (clone CS0DJ001YB09), melanotic melanoma (clone IMAGE:3916292) and mammary adenocarcinoma cell lines (clone IMAGE:5406358), and pooled primary tissues. (DR007866.1). Alignment of available Expressed Sequence Tags and cDNA sequences was used to generate a predicted mRNA of 2087 nucleotides. This is longer than the automatically predicted mRNA present in the databases (Locus XR_040412, 1158 nucleotides) because of the presence of 5′-UTR (178 nucleotides) and 3′-UTR (929 nucleotides) sequences. The intron-exon boundaries were defined by aligning the predicted mRNA to human genomic sequences. Fragments of the predicted mRNA were amplified by polymerase chain reaction (PCR) and sequenced to verify expression of this locus in HeLa cells. Real time PCR was used to detect expression of Idas in different human cell lines. The full predicted open reading frame (ORF) was amplified from HeLa cDNA and sequenced. The hIdas protein sequence was derived from the ORF. Idas orthologues in mouse (LOC622408) and *Xenopus laevis* (LOC100158359) were identified by Blast using the human Idas protein sequence as query. For sequence analysis and alignments, the following programs were used: Gene2EST (24), Coils (25), ELM (Eukaryotic Linear Motif) resource for functional sites in proteins (26), and ClustalW (27).

Plasmids—Total HeLa cDNA was used to amplify the hIdas ORF by nested PCR, introducing NheI and KpnI sites at the ends of the predicted hIdas ORF. The PCR product was cloned into the mammalian expression vector cDNA3.1EGFP (Invitrogen) at the NheI and KpnI restriction sites to produce a protein C-terminally fused to green fluorescent protein (GFP) under the control of the constitutive CMV promoter. N-Idas (amino acids 1–127) and C-Idas (amino acids 131–385) were cloned into the NheI and HindIII sites of pcDNA3.1EGFP (Invitrogen) after PCR amplification from full-length Idas to introduce restriction sites. IdasHA and Idas-Cherry were generated by replacing GFP from the IdasGFP pcDNA3.1 construct with three repeats of the human influenza hemagglutinin epitope (HA) and sequences coding for Cherry (Clontech), respectively. All products produced by PCR were fully sequenced.

For *in vitro* experiments, the predicted folded domain (101–284, dIdas) and the coiled-coil domain (173–245, tIdas) were cloned for expression in the NKI-His-3C-LIC (for cleavable His-tag expression) and the NKI-LIC plasmids (for native versions). Because these plasmids are resistant to kanamycin and ampicillin, respectively, they allow for efficient co-expression experiments. The Idas sequence was analyzed using the ProteinCCD server (28), which was also used for the automated design of oligonucleotides suitable for PCR-based restriction and ligase-free cloning to the NKI-LIC vectors. A construct expressing full-length Geminin was cloned in the pET22b vector from Novagen. A construct for expressing human Cdt1 harboring residues (158–396, mini-Cdt1) was cloned in the pET28a vector (Novagen) with an N-terminal His tag. For antibody production, N-Idas was cloned into the NheI and HindIII sites of pET28a vector (Novagen) with the N-terminal His tag using PCR amplification to introduce sites.

A mouse Idas cDNA (IMAGE: 5830438-C23) in vector pFLCI was obtained (Geneservice Ltd). A vector suitable for generation of antisense probes for *in situ* hybridization was constructed by removing the 3′-untranslated region of the cDNA using an internal KpnI site. A second vector for *in situ* hybridization was generated by subcloning the mIdas open reading frame to pBluescript between SacI and KpnI sites. The following plasmids have been described elsewhere: GeminGFP (29), GeminΔ90–120GFP (30, 31), Cdt1dhcRed (31), GeminHA (29), plasmids for mouse Geminin *in situ* probes (32, 33).

Real Time PCR—Idas mRNA expression levels were assessed by quantitative real time PCR (LightCycler 02, Roche Applied Science) using the QuantiFast SYBR Green PCR kit (204052, Qiagen). The primer sequences for Idas are 5′-GACGCGCTTGTTGAGAATAA-3′ and 5′-CACGTTCCGCTCCTTGAG-3′. Total mRNA was isolated using the RNeasy mini kit (74104,Qiagen), and 800 ng of total RNA were converted to cDNA using Superscript II (18064-014, Invitrogen).

A final dilution of 1:5 from the resulting cDNA was amplified for 40 cycles. All samples were normalized to the YWHAZ (tryptophan *5*-monooxygenase activation protein, ζ polypeptide) gene. The primer sequences for YWHAZ gene amplification are 5′-GATCCCCAATGCTTCACAAG-3′ and 5′-TGCTTGTTGTGACTGATCGAC-3′.

Cell Culture, Synchronization, and Transfections—HeLa and 293T cells were grown in DMEM (Invitrogen) with 10% fetal bovine serum (Invitrogen). MCF7 cells were grown in DMEM (Invitrogen) with 20% fetal bovine serum (Invitrogen). MCF7 ($1–3 \times 10^5$ cells) were transfected with a total of 1 μg of plasmid DNA using Genejammer (Stratagene) following the manufacturer's instructions, and cells were analyzed 22 h post-transfection. 293T cells were transfected using the calcium phosphate method. For the construction of stable cell lines expressing IdasGFP, HeLa cells were transfected with IdasGFP vector using Genejammer (Stratagene) and grown in the presence of Geneticin (500 μg/ml, 10131-019, Invitrogen). Resistant colonies were selected, screened for expression, and amplified.

For RNAi experiments, the following STEALTH (Invitrogen) siRNAs were used for Idas: 5′-CCACCAAACGGAAGCAGACTTCAAT-3′ and 5′-GAGACGCGCTTGTTGAGAATAATCA-3′. The negative control was 5′-CCAAACAGGAACGGACATTCCCAAT-3′. For Idas silencing, HeLa cells were treated with 50 nM concentrations of each Idas siRNA or 100 nM control siRNA twice (at 0 and 24 h) using Lipofectamine 2000 (Invitrogen) according to the manufacturer's instructions and were analyzed 24 h after the second transfection.

For mitotic synchronization, HeLa cells and 293T cells were incubated with nocodazole (50 ng/ml, Sigma) for 16 h. When synchronization was combined with transient transfection in HeLa or 293T cells, nocodazole was added 5 or 18 h after transfection, respectively.

Immunofluorescence, Immunohistochemistry—Cells grown on poly-lysine-covered coverslips were fixed in 4% paraformaldehyde for 10 min, washed twice with phosphate-buffered saline (PBS), permeabilized with 0.3% Triton X-100 in PBS, and

blocked in 3% bovine serum albumin and 10% fetal bovine serum in PBS (blocking solution) for 1 h. Coverslips were incubated with primary antibody in blocking solution overnight at 4 °C. Cells were washed with PBS, 0.1% Tween and incubated for 1 h with the following secondary antibodies in blocking solution: Alexa 488-conjugated goat anti-rabbit (A11034, Molecular Probes) and Alexa 568-conjugated goat anti-mouse (A11004, Molecular Probes). After washing, DNA was stained with DAPI or Hoechst.

For double immunostaining with BrdU, cells were first immunostained for Geminin or Cdt1 as above, fixed with 4% paraformaldehyde, and washed twice with PBS, 0.1% Tween followed by 1 h of incubation with 2 N HCl, washing with 0.1 M Tris-HCl, pH 8.8, and 1 h of blocking. Coverslips were incubated with anti-BrdU (1:80) (Oxford Biotechnology, OBT 00305) in blocking solution overnight at 4 °C, washed with PBS, 0.1% Tween, and incubated for 1 h with Alexa 568-conjugated goat anti-rat (A11077, Molecular Probes) secondary antibody in blocking solution. DNA was stained with Hoechst. Fluorescence immunohistochemistry was performed as described previously (33) on mouse embryos at E12.5 dpc.[2]

Non-radioactive *in situ* hybridization was performed as described in Spella *et al.* (33) on 10-μm sections of E12.5-dpc mouse embryos. For the generation of Idas antisense RNA probes, the pFLCI vector containing the mIdas open reading frame was first linearized with NotI and *in vitro* transcribed with T3 RNA polymerase. For control sense probe generation, the pBluescript vector containing the mIdas open reading frame was linearized with KpnI and transcribed with T7 RNA polymerase. Geminin sense and antisense probes were as described previously (32, 33). Sense probes were used as the control in all experiments. All animal-related procedures conformed to the international guidelines on the ethical use of animals. Images were recorded on a Nikon Eclipse TE 2000-U inverted microscope using 60×/1.40 oil and 40×/0.75 lenses.

Immunoprecipitation—MCF7 cells were transfected with the indicated plasmids and collected 22 h post-transfection. For immunoprecipitation of the endogenous proteins, total cell extracts were collected from HeLa cells. Total extracts were prepared by lysing cells in buffer containing 50 mM Tris-HCl, 150 mM NaCl, 5 mM EDTA, 0,5% Triton X-100, 5 mM $MgCl_2$, and protease inhibitors (1 mM phenylmethylsulfonyl fluoride, 2 mM benzamidine, 1 μg/μl leupeptin, 1.4 μg/μl pepstatin,1 μg/μl aprotinin, 1 μg/μl chymostatin, 0.1 M sodium vanadate). 1.5-μg antibodies bound to protein A-agarose beads (Upstate) were incubated with cell extracts for 3 h at 4 °C. After 3 washes with lysis buffer, immunoprecipitates and total cell extracts corresponding to 10% of immunoprecipitates were analyzed by Western blotting.

Antibodies—The following primary antibodies were used at the indicated dilutions. For immunofluorescence: rabbit anti-hIdas (hIdasAb2) (1:500), mouse monoclonal anti-Geminin (1:50) (32), rabbit anti-GFP (Molecular Probes, 1:2,000), mouse monoclonal anti-cyclin A (6E6,MS-1061–5, Neomarkers, 1:40), mouse monoclonal anti-cyclin B1 (GNS1, Santa Cruz, 1:200), and mouse monoclonal anti-α-tubulin (T5168, Sigma, 1:20,000). For immunohistochemistry: rabbit anti-hIdas (1:200) rabbit anti-Geminin (Ref. 32, 1:1500), mouse monoclonal anti-Pax6 (Developmental Studies Hybridoma Bank, University of Iowa, Iowa City, IA, 1:1,000). For immunoprecipitation: mouse monoclonal geminin (32), mouse monoclonal anti-GFP (3E6, 1181460001, Roche Applied Science), mouse monoclonal anti-HA (12CA5, sc-57592 Santa Cruz), and total mouse IgGs (Sigma). For Western blotting: rabbit anti-hIdas (hIdasAb1) (1:1000), rabbit anti-hIdas (hIdasAb2) (1:500) mouse monoclonal anti-actin (C4, Millipore, 1:3000), rabbit anti-Cdt1 (1:1000) (32), rabbit anti-Geminin (1:500) (32), rabbit anti-GFP (Santa Cruz, 1:500), and monoclonal anti-HA (12ca5, sc-57592 Santa Cruz, 1:500). Total human IgGs (Sigma) at 2 μg/ml were added to the blocking buffer to reduce binding of secondary antibodies to IgG chains and protein A/G present in immunoprecipitates.

Production of Recombinant N-Idas—N-Idas in pET28 vector was transformed in Rossetta cells (Novagen). Protein production was induced with isopropyl 1-thio-β-D-galactopyranoside (1 mM) at 37 °C at an optical density between 0.7–0.9 for 5 h. Cell pellets were sonicated in sonication buffer (300 mM NaCl, 50 mM Na_2HPO_4/H_2NaPO_4, 5 mM imidazole, 5 mM β-mercaptoethanol). After centrifugation, extracts were loaded on a nickel-nitrilotriacetic acid (Qiagen) column. N-Idas protein was eluted from the column at 500 mM imidazole, and dialyzed against 25 mM Tris, 50 mM NaCl buffer.

Production of Recombinant Geminin, Idas, and Complexes for in Vitro Analysis—Different Idas constructs were designed in ProteinCCD (28, 34), amplified by PCR, and inserted to the pETNKI-His-3C-LIC-kan vector. Vectors were transformed to Rosetta-2 cells (Novagen) and grown in the presence of a suitable antibiotic. For co-expression experiments, Idas plasmids were simultaneously transformed together with Geminin plasmids (23) in the presence of suitable antibiotics. Protein production was induced with isopropyl 1-thio-β-D-galactopyranoside at 15 °C at an optical density of ~0.8, and cells were left to grow for an additional 16–18 h at 15 °C. Cell pellets were obtained by centrifugation at 4000 rpm and lysed by sonication in 20 mM Hepes, pH 7.5, 200 mM NaCl, 5 mM β-mercaptoethanol (buffer A) plus a tablet of Complete, EDTA-free Protease Inhibitor Cocktail (Roche Applied Science) at 4 °C. After clearing the supernatant by centrifugation, the proteins were bound in a His-trap column (GE Healthcare) and eluted with a linear gradient of buffer A containing 20–500 mM imidazole. Fractions were analyzed by SDS-PAGE, and pure fractions were pooled. Yields were between 5–10 mg/liter of culture depending on the construct. All proteins were more than 95% pure as judged by SDS-PAGE (Fig. 3). All Idas-Geminin co-expression experiments were done with immobilized metal ion affinity chromatography purification mediated by the N-terminal histidine tag on Idas; in all purified complexes, stoichiometric amounts of Geminin were co-purified with Idas. All His tags were cleaved with 3C-protease before the characterization experiments. We were unable to obtain full-length Idas or its complexes in a soluble form suitable for biophysical experiments.

[2] The abbreviations used are: dpc, days post-coitus; NLS, nuclear localization signal; GEM, Geminin; D-box, destruction box; APC/C, Anaphase Promoting Complex/Cyclosome.

Antibody Production, Affinity Purification, and Antibody Characterization—dIdas and N-Idas recombinant proteins were used for rabbit immunizations (Harlan Sera-Lab) to generate antibodies hIdasAb1 and hIdasAb2, respectively. Crude sera were affinity-purified against the recombinant protein used for immunization. The specificity of the affinity purified antibodies were tested by Western blot analysis and shown to specifically recognize the hIdas protein in HeLa cells.

Analytical Size Exclusion Chromatography and Multiangle Laser Light Scattering—Experiments were performed in a Superdex 75 HR 10/30 column attached to an Akta FPLC and coupled to a miniDAWN light scattering detector (Wyatt Technology) and a Dn-1000 differential refractive index detector (WGE Dr. Bures). 100 μl of purified tIdas at a concentration of 0.3 mg/ml were injected to the column. Data analysis was carried out with the program Astra using a differential index of refraction value of 0.185.

Surface Plasmon Resonance Experiments—Surface plasmon resonance spectroscopy was preformed at 25 °C on a Biacore T100. About 6000 relative units of mini-Cdt1 and mini-Cdt1 Y170A were immobilized on a CM5 Chip (Biacore) at pH 5.5 using amino coupling of lysine residues. Concentrations series of all described Geminin and Idas variants and their complexes were injected across the chip in a buffer of 20 mM Hepes, pH 7.5, 200 mM NaCl, Tween 20 0.01% at a flow rate of 30 μl/min. The concentrations used were: 68, 200, 610, 1830, and 5500 nM for dIdas; 50, 151, 456, 1370, and 4100 nM for tIdas; 6, 19, 57, 170, 511, 1530, and 4600 nM for Geminin-dIdas; 13, 38, 113, 340, 102, 3060, and 9200 nM for Geminin-tIdas; 12, 36, 107, 322, and 967 nM for Geminin. Binding curves were recorded for each protein using the empty flow cell as reference. All experiments were repeated at least two times in a non-sequential manner to exclude systematic errors. The Biacore T100 evaluation software was used for the initial data analysis. All binding curves are shown in supplemental Fig. 2.

RESULTS

Idas, a Novel Coiled-coil Protein Related to Geminin—We searched human databases for Geminin homologues and identified the gene product of LOC345643, on chromosome 5q11.2, as being similar to Geminin in its central coiled-coil region. We named this gene *Idas*. *Idas* has 7 exons (supplemental Fig. 1*A*) and codes for a previously uncharacterized protein of 385 amino acids containing a putative coiled-coil region. *Idas* orthologues can be detected in different vertebrates. A multiple sequence alignment of Geminin orthologues with Idas orthologues from human, mouse, and *Xenopus* is shown in Fig. 1*A*. Geminin and Idas exhibit low overall similarity but significant conservation in their central coiled-coil regions, where the human Idas and Geminin proteins share 53% identity (Fig. 1*A*, *black box*). The central region of Geminin, which is conserved in Idas, mediates Geminin homodimerization and binding to Cdt1 (20–23). The Geminin coiled-coil has unique properties, with three polar residues in a and d positions of the heptad repeats, which are also present in Idas (Fig. 1*A*, *arrowheads*), suggesting that Idas may both homodimerize and heterodimerize with Geminin. Geminin-Cdt1 interactions were analyzed by PISA (35) based on the structure of the human Geminin-Cdt1 complex (PDB code 2WVR (23)). In Fig. 1*A*, Geminin residues important for Cdt1 binding are marked. The primary Cdt1-Geminin binding interface at the N-terminal region of the Geminin coiled-coil is partly conserved in Idas, whereas a second interface preceding the coiled-coil region of Geminin is not conserved.

A second region of weak conservation between Idas and Geminin can be detected at the N-terminal end of both proteins (Fig. 1*A*, *gray box*), encompassing the Geminin destruction box (D-box). The D-box, present in APC/C targets like Geminin, mediates interactions with APC/C activator subunits (36). Although the R*XX*L motif of the Geminin D-box is not conserved in the Idas orthologues, a R*XXLXX*P motif is present further N-terminally in hIdas (amino acids 27–31), suggesting that hIdas may also be regulated by APC/C mediated proteolysis. In the hIdas C terminus, two groups of basic amino acids (Fig. 1*A*) could function as nuclear localization signals (NLS). A typical bipartite NLS is present in this region in *Xenopus* Idas. At the C-terminal end of Idas, a region highly conserved between Idas orthologues is detected (Fig. 1*A*, *red box*). Idas is, therefore, a phylogenetically conserved coiled-coil protein with a sequence similarity to geminin.

Idas Is a Nuclear Protein and Associates with Geminin but Not with Cdt1—Idas mRNA expression is supported by five sequenced cDNAs (see "Experimental Procedures") and is detected by real time PCR in several cancer cell lines tested (data not shown). We amplified the *hIdas* coding sequence from HeLa cDNA and cloned it into a mammalian expression vector. Three constructs C-terminally fused to the GFP, were made: full-length Idas (amino acids 1–385, IdasGFP), an N-terminal fragment of Idas (N-IdasGFP, amino acids 1–127) containing the putative D-box domain, and a C-terminal fragment (C-IdasGFP, amino acids 131–385), containing the coiled-coil domain. The subcellular localization of Idas was assessed after transient transfection in MCF7 cells (Fig. 1*B*). IdasGFP and C-IdasGFP localize to the nucleus and are excluded from the nucleoli, similar to endogenous Geminin. In contrast, N-IdasGFP shows diffuse localization throughout the cell, consistent with the presence of a putative NLS at the hIdas C terminus.

Sequence analysis suggested that Idas could associate with Geminin and/or Cdt1. To test the ability of Idas to interact with Geminin in cells, MCF7 cells were co-transfected with IdasHA and GeminingFP or GeminΔ90–120GFP (a Geminin mutant lacking a significant part of the coiled-coil), and IdasHA was immunoprecipitated. As shown in Fig. 2*A*, GeminingFP, but not GeminΔ90–120GFP, was detected in the IdasHA immunoprecipitates. Consistently, in the reverse experiment, where GemininHA was used to immunoprecipitate Idas variants, IdasGFP and C-IdasGFP were detected in the immunoprecipitate, whereas N-IdasGFP, which lacks the Idas coiled-coil region, was not (supplemental Fig. 2*A*). These indicate that Geminin and Idas can form a complex in cells and that the coiled-coil regions of both proteins are required for this interaction.

To assess whether endogenous Idas and Geminin proteins are able to interact, we generated a specific antibody against hIdas (hIdasAb1) that recognizes a band of the correct molecular weight in HeLa cell extracts (data not shown; also, see

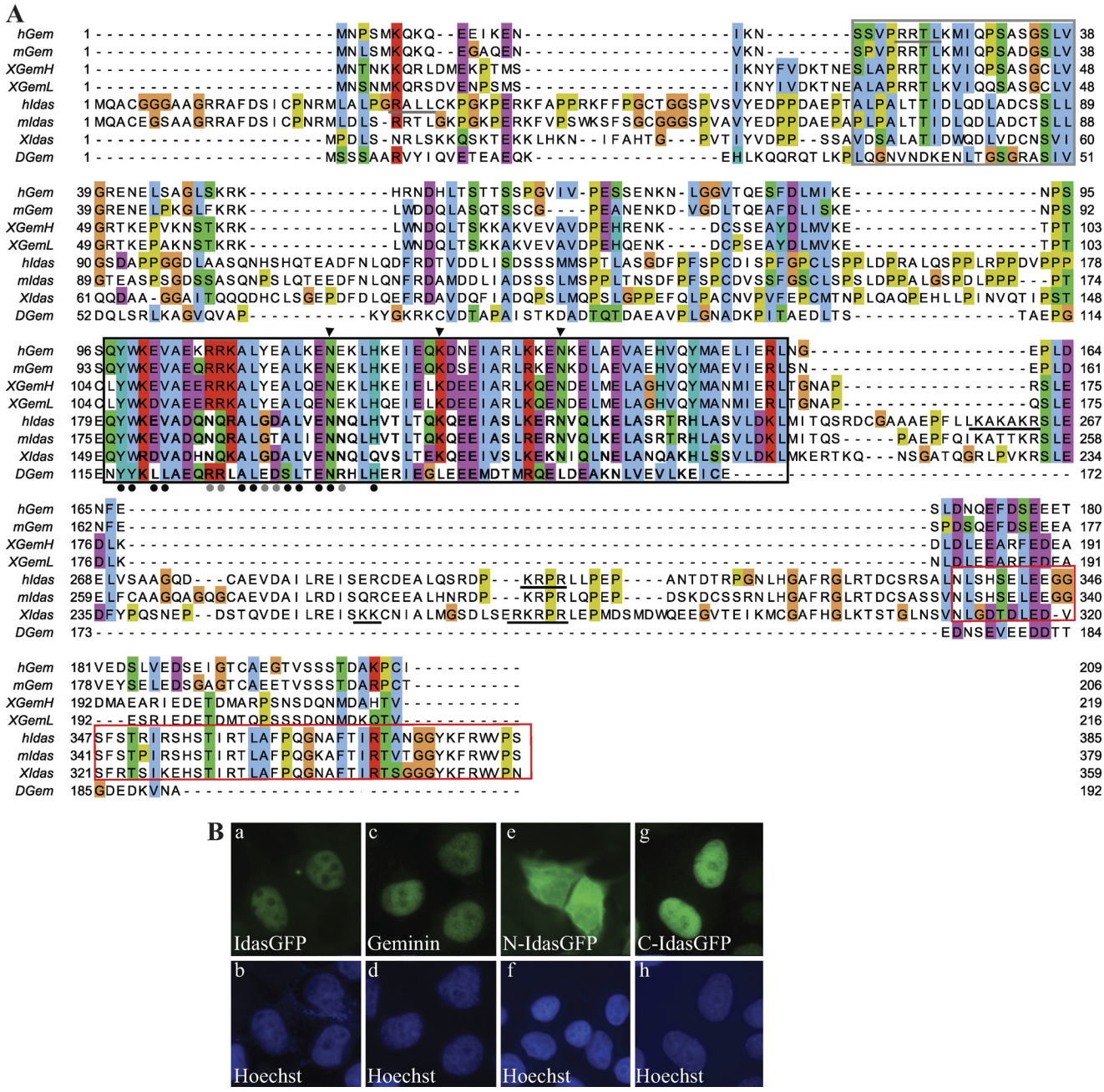

FIGURE 1. **Idas is a nuclear protein related to Geminin.** *A*, multiple sequence alignment of Geminin in human, mouse, *Xenopus*, and *Drosophila* with the predicted Idas sequences in human, mouse, and *Xenopus* is shown. *Black box*, conserved coiled-coil region; *red box*, conserved C-terminal region; *gray box*, D-box region. Putative D-box (*gray*) and NLS (*black*) are *underlined*. Polar residues in a and d coiled-coil positions are marked by *arrowheads*, and residues important for Cdt1 binding by *dots* (*black*, conserved in Idas; *gray*, not conserved). *B*, MCF7 cells were transfected with IdasGFP (*a* and *b*), N-IdasGFP (*e* and *f*), and C-IdasGFP (*g* and *h*). Immunofluorescence of endogenous Geminin is shown for comparison (*c* and *d*). DNA was stained with Hoechst.

later). Total cell lysates were immunoprecipitated with a Geminin-specific monoclonal antibody (Fig. 2*B*), and the presence of endogenous Idas in Geminin immunoprecipitates was assessed using the anti-Idas-specific antibody. Indeed, Idas is specifically detected in anti-Geminin immunoprecipitates (Fig. 2*B*, *lanes 4* and *5*). Conversely, endogenous Geminin is detected in an anti-Idas immunoprecipitate (supplemental Fig. 2*B*). These data taken together clearly indicate that endogenous Idas and Geminin interact in human cells.

We next tested the ability of Idas to self-associate by co-transfecting MCF7 cells with IdasGFP and IdasHA. IdasGFP specifically co-precipitated with IdasHA (Fig. 2*C*, *lane 6*), suggesting that Idas-Idas complexes can form in cells. The amount of IdasGFP immunoprecipitated with IdasHA, however, appeared relatively less compared with GeminGFP (*lane 5*), suggestive of a weaker interaction. We, therefore, assessed the ability of IdasHA to precipitate IdasGFP in the presence of co-transfected GeminGFP. IdasGFP was not detected in an IdasHA immunoprecipitate when GeminGFP was present

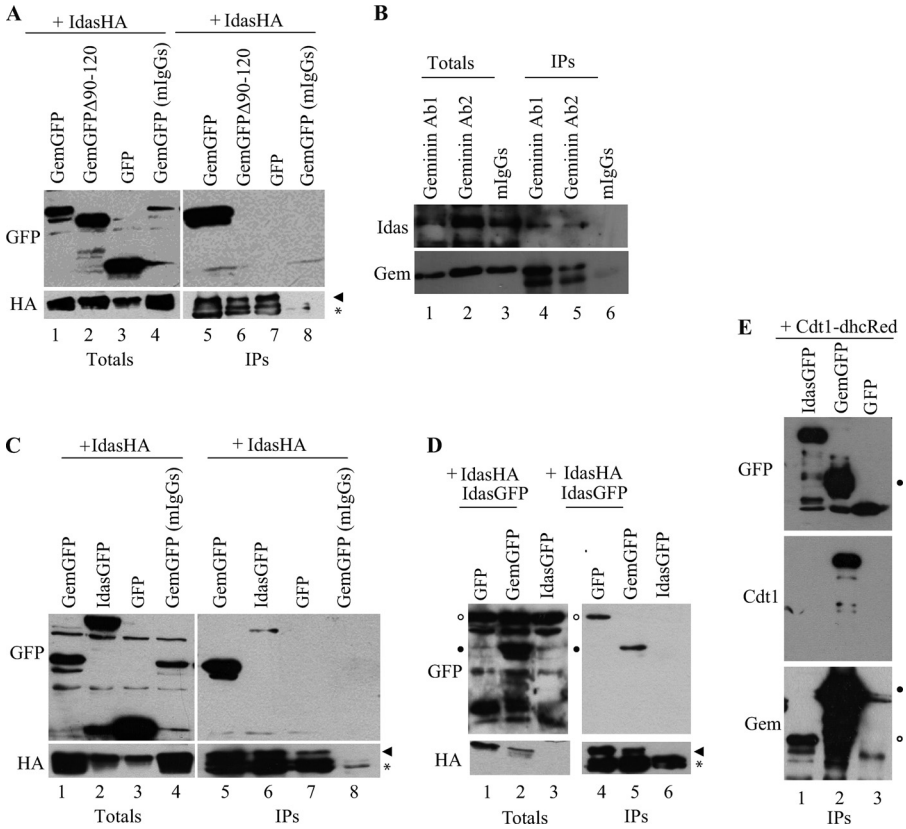

FIGURE 2. **Idas interacts with Geminin in cell extracts.** *A*, Geminin interacts with Idas through its coiled coil. MCF7 cells were co-transfected with IdasHA and GemininGFP (*lanes 1* and *5*), Geminin Δ90–120 GFP (*lanes 2* and *6*), or GFP (*lanes 3* and *7*). Total extracts (*Totals*, *left*) and anti-HA immunoprecipitates (*IPs*, *right*) were immunoblotted for GFP (*upper*) and HA (*lower*). *Lanes 4* and *8*, control immunoprecipitation of IdasHA-GemininGFP transfected cells with mouse IgGs. *B*, endogenous Geminin-Idas interaction is shown. Total cell extracts from HeLa cells were immunoprecipitated with two different purifications of an anti-Geminin mouse monoclonal antibody (*lanes 4* and *5*). Total lysates and immunoprecipitates were immunoblotted for Idas (*upper panel*) and Geminin (*lower panel*). Mouse IgG (*mIgG*) immunoprecipitates were used as a negative control. *C*, Idas self-associates. MCF7 cells were co-transfected with IdasHA and GemininGFP (*lanes 1* and *5*), IdasGFP (*lanes 2* and *6*), or GFP (*lanes 3* and *7*). Total cells lysates (*left*) and anti-HA immunoprecipitates (*right*) were immunoblotted for GFP and HA. *Lanes 4* and *8*, control immunoprecipitation with mouse IgGs. *D*, Geminin competes for Idas-Idas interactions. MCF7 cells were co-transfected with IdasHA, IdasGFP and GFP (*lanes 1* and *4*) or with IdasHA, IdasGFP, and GemininGFP (*lanes 2* and 5). Total cell lysates (*left*) and anti-HA immunoprecipitates (*right*) were immunoblotted for GFP (*upper*) and HA (*lower*). *Open circle*, IdasGFP; *filled circle*, GemininGFP. *Lanes 3* and *6*, transfection with IdasGFP alone (control). *E*, Idas does not interact with Cdt1. MCF7 cells were co-transfected with Cdt1-dhcRed and IdasGFP (*lane 1*), GemininGFP (*lane 2*), or GFP (*lane 3*). Anti-GFP immunoprecipitates were immunoblotted for GFP (*upper*), Cdt1 (*middle*), and Geminin (*lower*). *Open circle*, endogenous Geminin; *filled circle*, GemininGFP.

(Fig. 2*D*), suggesting that Geminin is the preferred partner of Idas in cells.

We then addressed whether Idas forms a complex with Cdt1 in cells similar to Geminin. Co-transfected Cdt1dhcRED could not be detected in an IdasGFP immunoprecipitate, whereas it was present in a GemininGFP immunoprecipitate (Fig. 2*E*). Endogenous Geminin was present in the IdasGFP immunoprecipitate, suggesting that Geminin, when in complex with Idas, does not bind to Cdt1. This suggests that Idas and Idas-Geminin complexes do not interact with Cdt1 in cells.

Our data suggest balanced Idas-Idas and Idas-Geminin interactions in cells, mediated through the homologous central coiled-coil regions of both proteins. Idas-Cdt1 complexes, however, could not be detected, suggesting that Idas binding to Geminin could affect Geminin-Cdt1 interactions.

Idas Binds Directly to Geminin, Reducing Its Affinity for Cdt1—To extend our findings in cells with studies *in vitro*, two variants of Idas, a large domain (amino acids 101–284, dIdas) and the coiled-coil region (amino acids 173–245, tIdas) were expressed in *Escherichia coli* (Fig. 3*A*). The absolute molecular mass of tIdas in the native state was determined by multiangle laser light scattering at 18,530 ± 500 daltons. This is consistent with a dimer of tIdas and shows that the coiled-coil region of Idas is sufficient for homodimerization.

Next, dIdas and tIdas were co-expressed in *E. coli* with full-length Geminin (Gem) and a truncated version that still binds Cdt1 and effectively inhibits licensing (amino acids 82–161, tGem). Idas and Geminin co-purified as tight complexes that were clearly stoichiometric, containing equal amounts of each protein (Fig. 3, *A* and *B*). Notably, the tGem-tIdas complex behaves as a tight, stoichiometric complex (Fig. 3*B*), suggesting that the Geminin and Idas coiled coils are not only necessary but also sufficient for tight interaction.

To investigate if Idas would bind to Cdt1 *in vitro* or if it would directly interfere with Geminin-Cdt1 binding, the affinities of Geminin, Idas, and their complexes to Cdt1 were assessed by surface plasmon resonance. A truncated version of human Cdt1 (residues 158–396, mini-Cdt1) and a mutant Cdt1 version (miniCdt1Y170A, in which a crucial tyrosine in the primary interface with Geminin was changed to alanine) were used. As shown in Fig. 3*C* and supplemental Fig. 3, Geminin exhibited an affinity to immobilized mini-Cdt1 of ~90 nM,

whereas its affinity to miniCdt1Y170A was lower by a factor of two (184 nM), suggesting that the assay is specific for interactions in the primary Geminin-Cdt1 interface. In contrast to Geminin, dIdas exhibited binding reduced by 2 orders of magnitude (7 μM) to both mini-Cdt1 and the Y170A mutant, whereas tIdas alone showed no detectable binding to Cdt1. This is consistent with the finding that Idas does not interact with Cdt1 in cell extracts. When Geminin was complexed with either dIdas or tIdas, Geminin binding to Cdt1 was reduced by at least 2 orders of magnitude (16 and 5 μM, respectively). Therefore, Idas associates with Geminin but not with Cdt1 *in vitro*, and Geminin-Idas complexes show severely reduced affinity for Cdt1. Moreover, the coiled-coil domain of Idas alone is sufficient to significantly inhibit Geminin binding to Cdt1. Our data show that Idas directly associates with Geminin through its coiled-coil region, forming a tight stoichiometric Idas-Geminin complex, and inhibits Geminin binding to Cdt1.

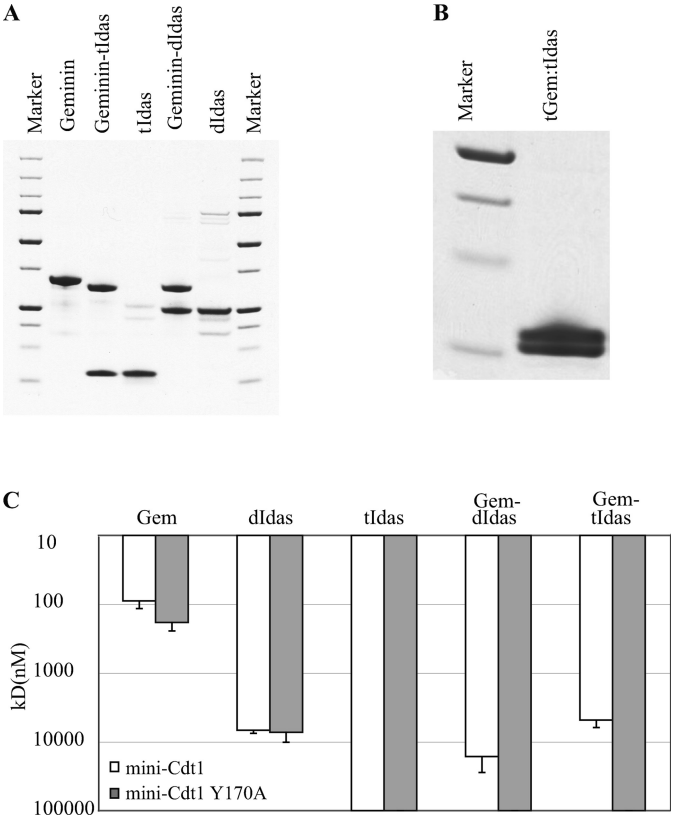

FIGURE 3. **Idas directly binds to Geminin *in vitro* and prevents Geminin from binding Cdt1.** *A* and *B*, polyacrylamide SDS-PAGE electrophoresis of Geminin, tIdas, dIdas, and Geminin-tIdas (*A*) and tGeminin-tIdas (*B*) complexes expressed and purified from *E. coli* is shown. *C*, quantification of Geminin and Idas affinities for Cdt1 by surface plasmon resonance is shown. The measured binding affinities of Geminin, dIdas, tIdas, Geminin-dIdas, and Geminin-tIdas complexes to mini-Cdt1 and mini-Cdt1Y170A immobilized on a Biacore T100 chip are shown.

Idas Affects Geminin Localization—Given the ability of Idas to form complexes with Geminin, we investigated whether it affects Geminin behavior in cells. hGeminin localizes to the cytoplasm when ectopically expressed in human cells (37). To study whether Idas can affect Geminin subcellular localization, MCF7 cells were co-transfected with GemininGFP and Idas-Cherry. As shown in Fig. 4, *A* and *B*, contrary to control cells where GemininGFP is excluded from the nucleus in 45% of transfected cells, in cells where Idas is co-expressed Geminin is nuclear, suggesting that Idas translocates Geminin to the nucleus. These data indicate that Idas can form a complex with Geminin within live cells and affect Geminin cellular behavior. Nuclear import of Geminin is essential for its function in *Xenopus* (38).

Idas Depletion Prevents Normal Cell Cycle Progression—To assess if Idas is implicated in the cell cycle, RNA interference was performed to silence the expression of Idas in HeLa cells. Cells were treated with RNAi, and 48 h post-transfection mRNA levels were assessed by real time RT-PCR (Fig. 5*A*). A 10-fold decrease in Idas mRNA was detected in Idas siRNA-transfected cells compared with control transfected cells (Fig. 5*A*). As shown in Fig. 5*A*, *inset*, Idas protein was undetectable after the siRNA treatment compared with control-treated cells, consistent with the efficient knockdown of Idas shown by RT-PCR.

Cells depleted of Idas showed an increase in the percentage of BrdU-incorporating cells (38.5 $\pm$ 4.2% compared with 22.9 $\pm$ 3.2% positive cells in control; Fig. 5*C*) corresponding to a 1.68-fold increase (Fig. 5*B*). The increased BrdU incorporation in Idas RNAi-transfected cells was accompanied with a 1.4-fold increase in Geminin-positive cells (48.4 $\pm$ 3.8% compared with 34.4 $\pm$ 4.3% positive cells in control) and a 0.7-fold reduction in Cdt1-positive cells (36 $\pm$ 6.5% compared with 49 $\pm$ 7.5% positive cells in control, Fig. 5, *B* and *C*). Geminin marks the S and G_2 phases (2), whereas Cdt1 marks the G_1 phase of the cell cycle (5). The above results indicate that Idas depletion affects the cell cycle, leading to an increased fraction of cells in S phase.

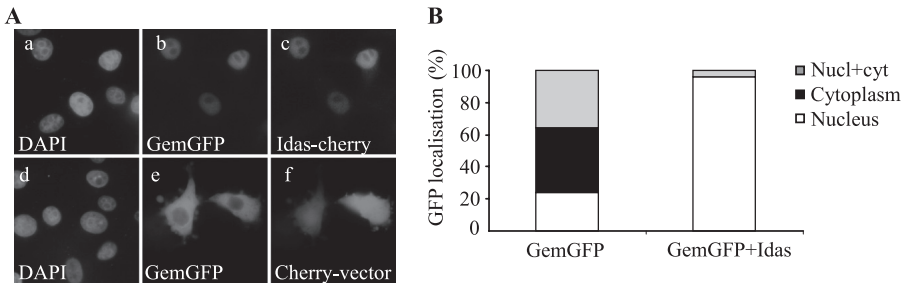

FIGURE 4. **Idas targets Geminin to the nucleus.** *A*, MCF7 cells were co-transfected with GemininGFP and Idas-Cherry (*upper*) or Cherry vector (*lower*), and the subcellular localization of GFP (*b* and *e*) and Cherry (*c* and *f*) was assessed. DNA was stained with DAPI (*a* and *d*). *B*, quantification of GemininGFP subcellular localization after co-transfection with Idas-Cherry (*right*) or Cherry (*left*, control) is shown. *Nucl*, nucleus; *cyt*, cytoplasm.

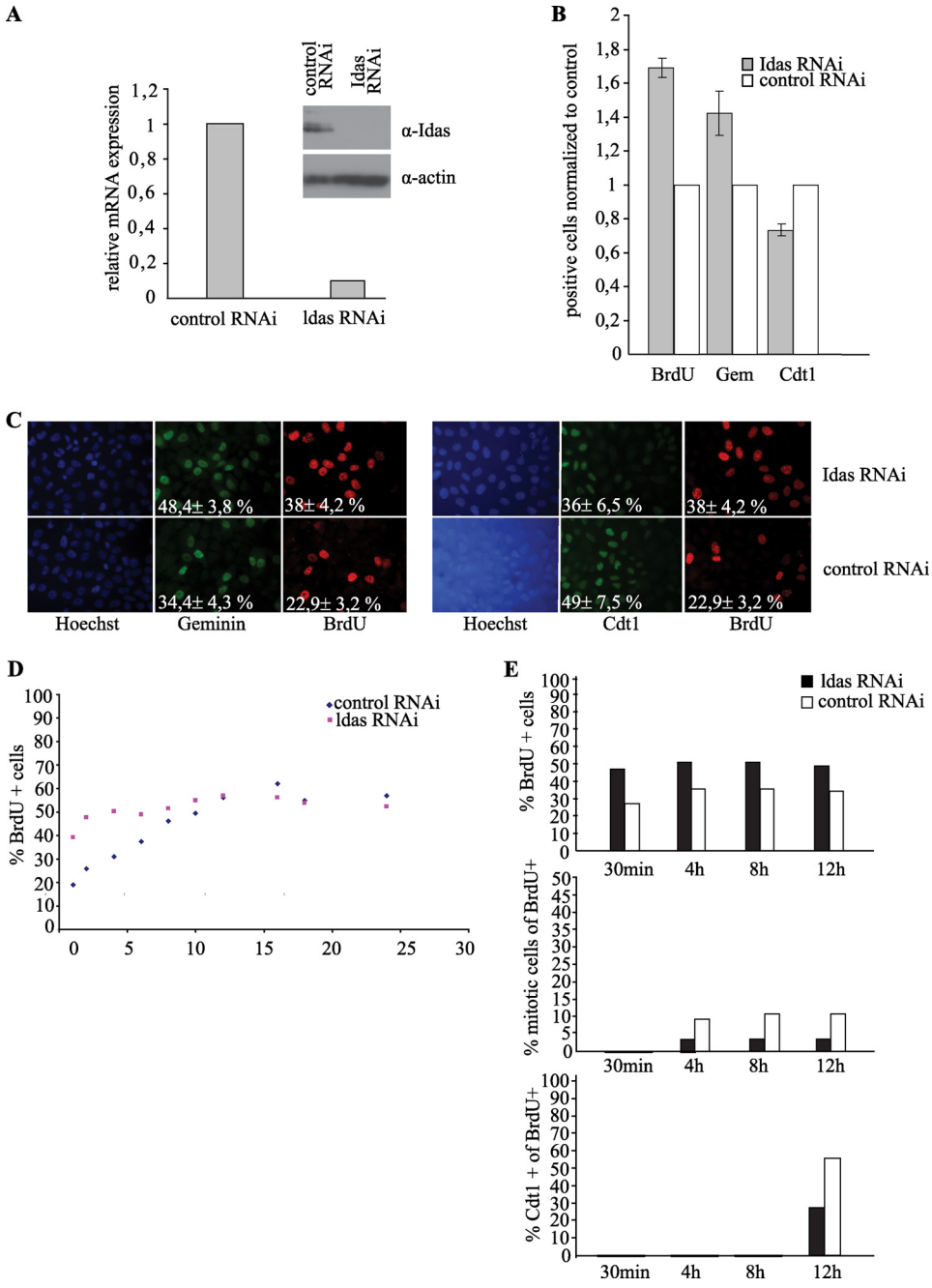

FIGURE 5. **Idas RNAi prevents normal cell cycle progression.** *A*, quantification of Idas mRNA and protein levels in HeLa cells after Idas RNAi, relative to control RNAi, by real time PCR (*graph*) and Western blot analysis using an Idas-specific antibody (*inset*, hIdasAb1) 48 h post-transfection. *B* and *C*, HeLa cells were transfected with Idas siRNA or control siRNA and 48 h post-transfection pulsed with BrdU for 30 min, fixed, and immunolabeled with anti-BrdU and anti-Geminin or anti-Cdt1 antibodies. DNA was stained with Hoechst. Quantification of cells positively stained for BrdU, Geminin, and Cdt1 in Idas siRNA-treated normalized to control-treated HeLa cells is shown in *B*. For each experiment, the % positive cells in control-treated cells was set to 1. -Fold increase/decrease is shown as a mean of three independent experiments, with S.D. More than 400 cells were measured for each experiment. Representative images are shown in *C*, with % positive cells ±S.D. indicated in each image. *D*, HeLa cells were treated with Idas or control siRNA and 48 h post-transfection were treated with BrdU for a total of 24 h. Time points were collected at 1, 2, 4, 6, 8, 10, 12, 16, 18, and 24 h after BrdU addition. Cells were fixed and stained with anti-BrdU antibody. DNA was stained with Hoechst. The BrdU labeling index was plotted against the BrdU pulse time. *E*, HeLa cells were treated with Idas or control siRNA, and 48 h post-transfection cells were treated with BrdU for 30 min, then BrdU was washed out, and cells were left in a BrdU-free medium. After BrdU removal, time points were collected at 30 min and 4, 8, and 12 h. Cells were fixed and immunolabeled with anti-BrdU and anti-Cdt1 antibodies. DNA was stained with Hoechst. The percentage of all cells scoring positive for BrdU (*upper*) and the percentage of BrdU-positive cells that show mitotic nuclear morphology (*middle*) or are positive for Cdt1 (*bottom*) are plotted at each time point to determine progression into Mitosis and G_1 phase, respectively.

To understand if the increase in the fraction of cell in S phase after Idas depletion is due to an extended S phase, HeLa cells treated with Idas siRNA or control siRNA were incubated in the presence of BrdU for a total period of 24 h, and time points were collected. The BrdU labeling index is plotted against the BrdU incubation time (Fig. 5*D*). Both control and Idas siRNA-treated cells showed a similar in-cycle pool, as the fraction of cells incorporating BrdU at long time points was similar. In contrast to control-treated cells, however, which showed a constantly increasing number of cells incorporating BrdU and entering S

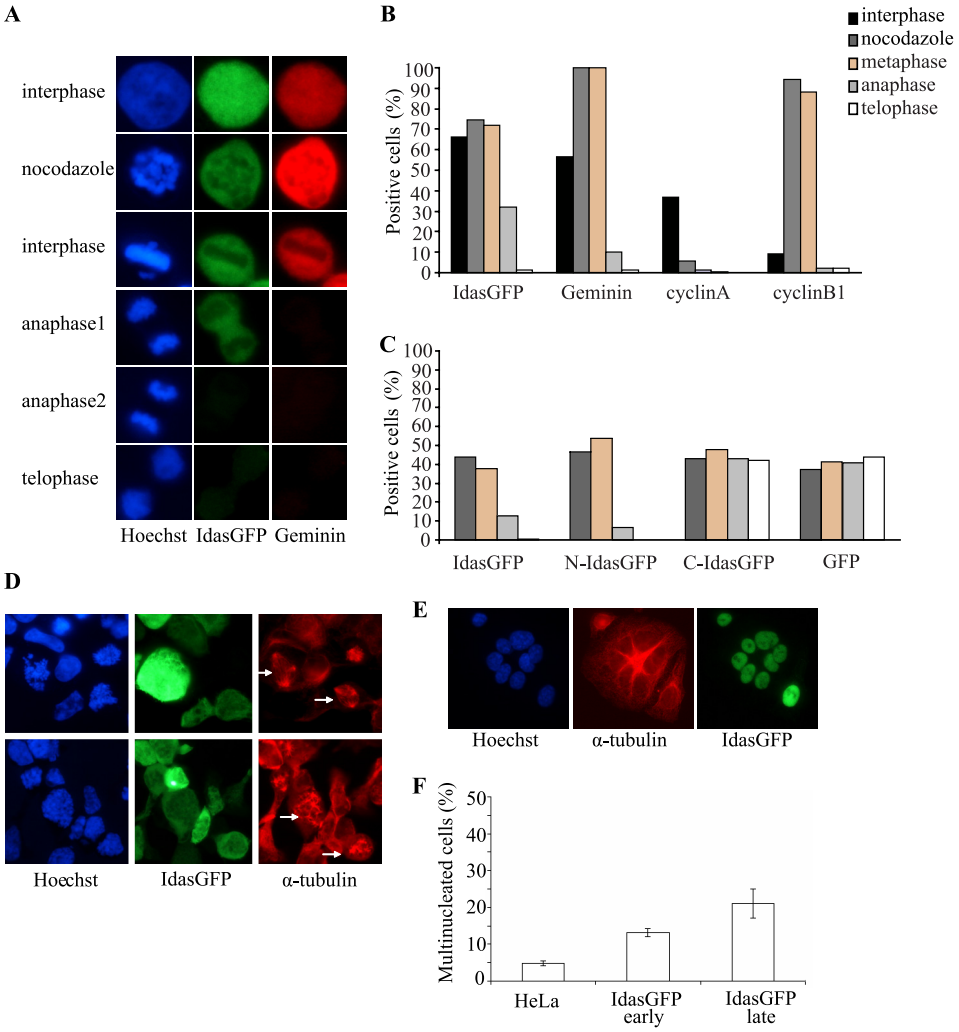

FIGURE 6. *A*, Idas is degraded during anaphase. HeLa cells stably expressing IdasGFP were synchronized in mitosis by nocodazole, released, and GFP (*middle*) and Geminin (*right*) were detected by immunofluorescence. Cells are arranged by mitotic stage based on Hoechst staining. *B*, quantification of IdasGFP-, Geminin-, Cyclin A-, and Cyclin B1-expressing cells by mitotic stage is shown. See supplemental Fig. 3 for images. *C*, 293 T cells transfected with IdasGFP, N-IdasGFP, C-IdasGFP, or GFP were arrested in mitosis by nocodazole and released, and the % of cells expressing GFP in different mitotic stages was assessed. See supplemental Fig. 3 for images. *D*, Idas overexpression causes mitotic defects. 293 T cells were transfected with IdasGFP or GFP as control and treated with nocodazole for 16 h. After release, double immunofluorescence for α-tubulin and GFP was carried out. Examples of cells with abnormal spindles observed after IdasGFP transfection are shown. *E*, different passages of HeLa cells stably expressing Idas-GFP were stained for GFP and α-tubulin. Multinuclear giant cells were observed (*E*) and quantified (*F*). Parental HeLa cells were used as control.

phase until ~12 h, a very small increase in BrdU incorporation against pulse time was observed in Idas siRNA-treated cells (Fig. 5*D*), showing that almost all cycling cells are in S phase from the first time points. We, therefore, conclude that in the absence of Idas, the majority of cycling cells accumulate in S-phase.

To address whether cells accumulating in S-phase in the absence of Idas are able to efficiently exit S phase and progress in the cell cycle, we used a short-pulse BrdU and chase assay. Control-treated and Idas RNAi-treated cells were pulsed with BrdU for 30 min, then BrdU was washed out, cells were incubated in a BrdU-free medium, and time-points were collected for a period of 12 h. The fraction of BrdU-stained cells showing a mitotic nuclear morphology was used as an indication of entry into mitosis, whereas Cdt1 was used as a G_1 phase-specific marker. As shown in Fig. 5*E*, in contrast to control-treated cells, Idas siRNA-treated cells show a reduced ability to enter mitosis and G_1. The above results indicate that Idas depletion from HeLa cells results in cells accumulating in S-phase but unable to efficiently progress to mitosis and G_1, suggestive of S phase defects. This is consistent with a role of Idas in modulating cell cycle progression and is reminiscent of Geminin overexpression experiments in certain cell types (14).

Idas Levels Decrease in Anaphase, and Its Overexpression Causes Mitotic Defects—Given the presence of a putative D-box at the N terminus of Idas, we investigated whether Idas protein levels may be regulated during the cell cycle. A HeLa cell line stably expressing IdasGFP was generated. As IdasGFP is under the control of a constitutive promoter in these cells, post-transcriptional regulation of Idas can be assessed. These cells were synchronized in mitosis, and IdasGFP levels were assessed in parallel with Geminin (Fig. 6, *A* and *B*), Cyclin A (Fig. 6*B*, supplemental Fig. 3), and Cyclin B1 (Fig. 6*B*, supplemental Fig. 3). IdasGFP levels were high during most of interphase and early mitosis and sharply decreased during anaphase, whereas IdasGFP was undetectable during telophase and cytokinesis (Fig. 6,

A and *B*). IdasGFP accumulated again early in G_1 (data not shown). IdasGFP levels decrease after Cyclin A (which is degraded in prometaphase), Cyclin B1, and Geminin (which are degraded at the metaphase to anaphase transition (36)), suggesting that Idas is an APC/C target in anaphase. To investigate which part of the Idas protein mediates the observed anaphase-specific decrease, N-IdasGFP and C-IdasGFP were tested in parallel to full-length Idas-GFP and GFP control. As shown in Fig. 6*C* and supplemental Fig. 4, N-IdasGFP was degraded similar to full-length IdasGFP during anaphase, whereas C-IdasGFP protein levels remained stable during mitosis, similar to control GFP, showing that the first 130 residues of Idas are required and sufficient for its cell cycle-specific proteolysis.

Given the cell cycle-specific pattern of IdasGFP expression, effects of Idas overexpression on mitotic progression were assessed. The effect of short term high level overexpression of IdasGFP was studied by transiently transfecting IdasGFP in 293T cells. The level of overexpression was assessed by real time PCR, and Idas mRNA levels were found to be 3 orders of magnitude higher than endogenous Idas (data not shown). Cells with abnormal spindle formation (multipolar spindles) or irregular giant sizes could be observed in IdasGFP overexpressing cells more often than in control-transfected cells (Fig. 6*D*). The long term effect of Idas overexpression was studied in a HeLa cell line stably expressing IdasGFP. Idas expression in the stable cell line was found to be increased by 2 orders of magnitude compared with endogenous expression as assessed by real time PCR (data not shown). Multinucleated giant cells were observed in IdasGFP-expressing cells more frequently than in control HeLa cells (Fig. 6*E* and quantification in Fig. 6*F*). The number of multinuclear cells was further increased in later passages of the stable cell line (Fig. 6*F*). Therefore, ectopic expression of Idas interferes with normal mitotic progression. Geminin depletion has similarly been reported to cause mitotic defects and to give rise to multipolar spindles (12).

Idas Is Highly Expressed in Parts of the Developing Mouse Brain—To gain insight into the role of Idas at the organismal level, we examined its expression in the developing mouse embryo and compared it to the expression of Geminin. *In situ* hybridization experiments on mouse embryos at E12.5 dpc showed that Idas exhibits high level expression in a restricted pattern in the developing mouse brain. Idas transcripts were detected at high levels in the cortical hem and the choroid plexus epithelium (Fig. 7*Aa*) in the telencephalic midline. In contrast, Geminin mRNA was localized throughout the ventricular and subventricular zones of the embryonic telencephalon (Fig. 7*Ab*) where proliferating cells are localized, consistent with previous studies (33).

To study the expression of Idas at the protein level, an anti-hIdas-specific antibody suitable for immunofluorescence was generated (hIdasAb2). Immunofluorescence on mouse sections of an E12.5-dpc embryo for Idas protein revealed an expression pattern similar to its mRNA (Fig. 7*B*). Endogenous Idas localizes to the nucleus (Fig. 7*B*), similar to the overexpressed protein. Double immunofluorescence for Pax6 (Fig. 7*B*, *c* and *e*, *red*), a marker of neurogenic radial glial cells that constitutes a population of the telencephalic neural progenitor pool, indicates that Idas is expressed by cells starting to differentiate, whereas Geminin is predominantly expressed by neural progenitors. Endogenous Idas protein is detected at high levels by Western blotting in Z310 cells (Fig. 7*C*, *lane 4*), a rat choroid plexus-derived cell line, consistent with immunofluorescence and *in situ* hybridization results. In this cell line, where Idas is expressed at high levels, endogenous Idas can be detected in the nucleus by immunofluorescence and is excluded from the nucleoli (Fig. 7*D*). This is similar to ectopically expressed Idas (Fig. 1*B*) and consistent with immunofluorescence results using mouse sections (Fig. 7*B*).

Our results show that Idas mRNA and protein are detected at high levels in specific parts of the developing mouse brain. Expression in the medial wall of the telencephalon suggests an involvement in signaling events patterning the telencephalon. Balanced interactions of Geminin with Cdt1 and transcriptional modulators have been suggested to affect proliferation-differentiation decisions during neurogenesis (1, 17). The identification of Idas as a novel Geminin binding partner expressed in the developing brain, which is implicated in the cell cycle and can compete for Geminin-Cdt1 interactions, suggests a regulatory role for Idas in proliferation-differentiation decisions during neurogenesis.

DISCUSSION

The Geminin Superfamily—Geminin is a bifunctional molecule; it contributes to the maintenance of genomic stability by binding to Cdt1 and preventing rereplication (6) and also participates in cell fate choices during development (39). Geminin is conserved from *Caenorhabditis elegans* to human, whereas a Geminin analog has been proposed to exist in plants (40). Geminin is believed to regulate the transition from proliferating to post-mitotic-differentiated cells (16, 41). Given the above, Geminin has been proposed as a regulatory factor that has evolved at the transition from unicellularity to multicellularity (42). Geminin establishes its regulatory role through interactions with a number of binding partners. The coiled-coil domain of the protein is necessary for these interactions, either acting as a binding interface or maintaining the structural integrity of the molecule (39).

In this study we searched for proteins that share sequence and possible functional homology to Geminin. We describe a novel phylogenetically conserved coiled-coil protein named Idas. We show that Idas is expressed in human cells and in the developing mouse embryo. Although overall Idas and Geminin show low sequence similarity, they exhibit significant conservation between their coiled-coil domains, indicating that they are evolutionarily related. Idas orthologues can be identified in amphibia and fish but not in invertebrates (data not shown).

Recently, Balestrini *et al.* (43) characterized a different protein homologous to the Geminin coiled-coil that they named GEMC1. GEMC1 is implicated in the cell cycle and is required for DNA replication in *Xenopus* extracts. It was shown to interact with TopBP1 and to be a rate-limiting cyclin-dependent kinase target. Idas and GEMC1 possess two regions of significant similarity; that is, the coiled-coil region and the phylogenetically conserved C-terminal box (*black* and *red boxes* in Fig. 1*A*, identities 37 and 47%, respectively, shown in *purple* and *gray* in Fig. 7). Geminin does not possess the C-terminal con-

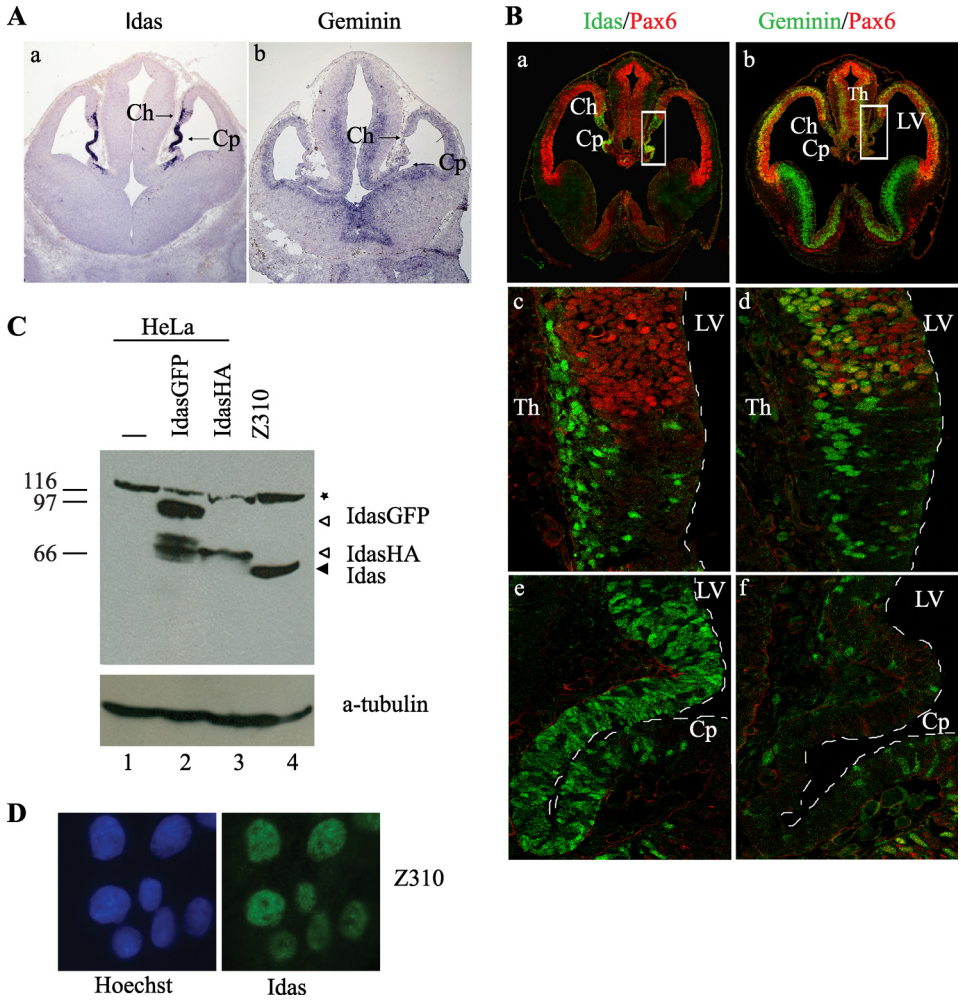

FIGURE 7. **Expression of Idas and Geminin in the developing mouse brain.** *A*, *in situ* hybridization for Idas (*a*) and Geminin (*b*) on an E12,5 dpc mouse embryo is shown. *B*, double immunofluorescence experiments for Idas (*green*, *a*, *c*, and *e*) and Geminin (*green*, *b*, *d*, and *f*) together with the radial glial marker Pax6 (*red*) on an E12.5 dpc mouse embryo are shown. *Boxed areas* in *a* and *b* are depicted in higher magnification in *c* and *e* and in *d* and *f*, respectively. Note the nuclear localization of Idas. *Ch*, cortical hem; *Cp*, choroid plexus; *LV*, lateral ventricle; *Th*, thalamus. *C*, shown is Western blot analysis of whole cell extracts from HeLa cells non-transfected (*lane 1*), transfected with IdasGFP (*lane 2*), or IdasHA (*lane 3*) and the choroid plexus derived Z310 cells (*lane 4*) using the anti-Idas specific antibody hIdasAb2. Anti-tubulin serves as a loading control. *Star*, nonspecific band. Endogenous Idas is not detectable in HeLa cells in this experiment due to its lower expression levels. *D*, Z310 cells were fixed and processed for immunofluorescence using the anti-hIdas hIdasAb2 antibody. Endogenous Idas appears in the nucleus excluded from the nucleoli.

served box shared between Idas and GEMC1. The Geminin and Idas coiled-coil regions, however, are more similar to each other than to the GEMC1 coiled coil. In particular, Geminin and Idas share a heptapeptide at the N-terminal end of the coiled coil (QYWKEVAE), not present on GEMC1. We could not detect Idas and GEMC1 orthologues in invertebrates, suggesting that Idas, Geminin, and GEMC1 may have arisen in vertebrates through duplication of an ancestral Geminin-like gene. Geminin, Idas, and GemC1 are, therefore, members of a Geminin superfamily that may have appeared during vertebrate evolution concomitantly with the increase of organism complexity, consisting of proteins important for normal cell cycle progression.

Idas Is a Nuclear Protein Regulated during the Cell Cycle—Idas protein is shown to localize to the nucleus and to be excluded from the nucleoli, exhibiting the same intracellular localization pattern as Geminin. This is observed with ectopically expressed GFP-tagged Idas but also for endogenous Idas in Z310 cells and in sections of the developing mouse brain. The C-terminal part of Idas (residues 128–385) is essential for Idas nuclear localization, consistent with the presence of two groups of basic amino acids in positions 259–264 and 301–304 of the C-terminal part of the protein, that could function as a bipartite NLS (44).

In a stable cell line generated for IdasGFP, Idas protein levels were found to decrease during anaphase and rise again in early G_1. The anaphase promoting complex has a key role in the recognition and degradation of protein substrates during mitosis and in G_1, recognizing the D box or KEN box on its substrates (45). At the N-terminal part of Idas, a RALL (residues 27–31) short sequence motif of the R*XX*L-type destruction box consensus sequence of mitotic cyclins could function as a D-box. Consistently, a mutant of Idas lacking the complete N-terminal part of the protein (residues 1–127), including the possible D-box, is not regulated during mitosis. Geminin is also an APC/C substrate during mitosis and G_1 (2). Idas protein levels appear to decrease soon after Geminin protein levels during anaphase. Interestingly, in addition to Geminin, positive

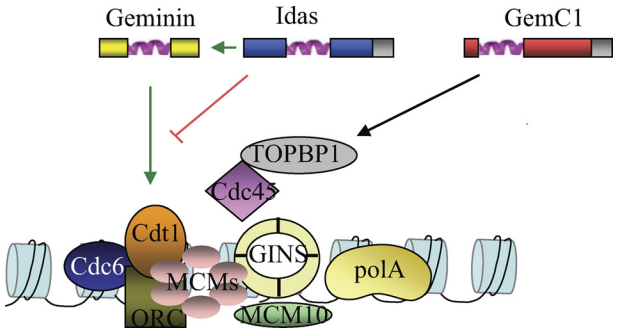

FIGURE 8. **The Geminin superfamily is implicated in the regulation of DNA replication.** Graphic representation of Geminin, Idas, and GEMC1 proteins share the Geminin like coiled-coil domain (shown in *purple*). Idas and GEMC1 also share a C-terminal conserved box (shown in *gray*) not present on Geminin. Idas interacts with Geminin and inhibits Geminin interactions with Cdt1. GEMC1 was shown to interact with TopBP1 and to regulate Cdc45 loading to chromatin (43). *MCM*, Mini-Chromosome Maintenance complex (MCM2–7); *ORC*, Origin Recognition Complex; *polA*, polymerase A.

regulators of pre-RC formation, such as Cdt1 and Cdc6, have also been found to be targets of the APC/C (46–48).

Idas Binds to Geminin Reducing Its Affinity for Cdt1—In this study we show that endogenous Idas and Geminin interact physiologically in human cells. *In vitro* data suggest that the Idas-Geminin interaction is direct, and a tight stoichiometric complex is formed. The coiled-coil regions of both proteins are sufficient for this interaction, as a tight stoichiometric complex is formed *in vitro* by the tIdas and tGeminin constructs, which only contain the coiled-coil regions of each protein. The high affinity of Idas-Geminin interactions is indicated by the fact that Idas self-association is inhibited in the presence of excess Geminin in cells, in favor of the formation of an Idas-Geminin complex. Idas-Geminin interactions occur in cells, as Idas can change the subcellular localization of Geminin upon co-transfection.

Interestingly, although several amino acids important for Cdt1 binding (20, 23) are conserved in the Idas coiled-coil region, Idas does not interact with Cdt1 either in cells or *in vitro*. This lack of interaction between Idas and Cdt1 highlights residues on the primary Geminin-Cdt1 interface that could be essential for a stable interaction. It may further be explained by the lack of the secondary binding interface that precedes the coiled-coil region of Geminin. On Idas, this region has been replaced with a proline-rich region (Fig. 1*A*).

Moreover, we show that Idas binding can reduce Geminin affinity for Cdt1. In surface plasmon resonance binding experiments, the ability of Geminin to bind Cdt1 in the presence of Idas is severely diminished. Taken together, our data suggest that Idas directly binds to Geminin and prevents it from binding to Cdt1 (Fig. 8). A balance between Geminin interactions with Cdt1 and transcriptional regulators has been suggested to affect cell fate decisions during differentiation (39). We describe here a novel protein that could affect these balanced interactions through direct binding to Geminin.

Idas Depletion and Overexpression Cause Cell Cycle Defects—To gain insight into Idas function in cells, we silenced Idas expression by siRNA-mediated knockdown in HeLa cells. Idas depletion resulted in an increased S phase population. In cumulative BrdU experiments, the majority of cycling Idas RNAi-treated cells were found to be accumulated in S phase. They were able to incorporate BrdU but unable to exit S phase, as in BrdU pulse-chase experiments Idas-depleted cells showed defective progression from S-phase to mitosis and G_1. The above results indicate the importance of Idas for normal cell cycle progression. Idas depletion could lead to precautious Geminin activation, mimicking Geminin ectopic expression, which also prevents normal cell cycle progression to mitosis due to an impaired S phase (8, 9, 14). We were, however, unable to reverse the Idas depletion phenotype by concomitant inactivation of Geminin (data not shown), suggesting that Idas may have additional partners in cells.

Cell cycle defects were also observed in Idas overexpression experiments. Both short and long term Idas overexpression resulted in abnormal mitotic phenotypes. In transient transfections, cells with multipolar spindles were observed, whereas an increased percentage of multinuclear cells were observed in cells stably expressing IdasGFP, possibly due to the accumulation of cells with spindle abnormalities. Geminin has also been implicated in normal progression through mitosis, as Geminin depletion was shown to cause centrosome over-duplication, resulting in multipolar spindles (12).

Idas Is Expressed to High Levels in the Developing Mouse Telencephalon—Geminin has a double function; it is essential for normal cell cycle progression by inhibiting Cdt1 but is also implicated in proliferation-differentiation decisions during development. To assess if Idas might also have additional functions during development, we investigated whether it is expressed at high levels in a tissue-specific manner during development.

In the developing mouse embryo, Idas was found to be specifically highly expressed in the cortical hem and choroid plexus of the developing mouse telencephalon, both at the mRNA and protein level. The endogenous protein was found to be in the nucleus, similar to Idas expressed in human cell lines. High levels of endogenous Idas were also detected in total cell extracts in a rat choroid plexus cell line, whereas nuclear localization of endogenous Idas was further verified in this cell line by immunofluorescence. The above results are consistent with a strong expression of Idas in specific parts of the mouse telencephalon. There is accumulating evidence that the telencephalic midline participates in signaling and patterning of the cortical neuroepithelium and the cerebellar cortex (49–52). Because Idas exhibits a strong expression in these domains, it could participate in signaling events patterning the telencephalon. The high level expression of Idas in a tissue-specific context supports the notion that Idas could be implicated in Geminin-mediated balanced interactions important for proliferation *versus* differentiation decisions during development (39).

In summary, in this study we introduce a novel Geminin partner, Idas, related in sequence to the Geminin coiled coil. Idas is a cell cycle-regulated protein that interacts with Geminin and reduces Geminin affinity for Cdt1 (Fig. 8). Geminin, Idas, and the recently described GEMC1 protein families may have arisen through functional divergence of duplicated gene products in vertebrates and may have related but distinct functions in modulating cell cycle progression and differentiation through balanced interactions.

Given its central role as a cell cycle regulator, Geminin has attracted significant attention for anti-tumor drug development (13, 14). We show here that the coiled-coil of Idas is a potent inhibitor of the Geminin-Cdt1 complex, suggesting that peptides deriving from Idas may provide a powerful means to modulate Geminin function in cells.

Acknowledgments—We thank A. Fish for help with surface plasmon resonance experiments, Martin Hasselblatt for kindly providing the Z310 cell line, and Maria Iliou for kindly providing the mouse monoclonal anti-Geminin antibody.

REFERENCES

1. Seo, S., and Kroll, K. L. (2006) *Cell Cycle.* **5,** 374–379
2. McGarry, T. J., and Kirschner, M. W. (1998) *Cell* **93,** 1043–1053
3. Wohlschlegel, J. A., Dwyer, B. T., Dhar, S. K., Cvetic, C., Walter, J. C., and Dutta, A. (2000) *Science* **290,** 2309–2312
4. Tada, S., Li, A., Maiorano, D., Méchali, M., and Blow, J. J. (2001) *Nat. Cell Biol.* **3,** 107–113
5. Nishitani, H., Taraviras, S., Lygerou, Z., and Nishimoto, T. (2001) *J. Biol. Chem.* **276,** 44905–44911
6. Blow, J. J., and Dutta, A. (2005) *Nat. Rev. Mol. Cell Biol.* **6,** 476–486
7. Lygerou, Z., and Nurse, P. (2000) *Science* **290,** 2271–2273
8. Zhu, W., Chen, Y., and Dutta, A. (2004) *Mol. Cell. Biol.* **24,** 7140–7150
9. Melixetian, M., Ballabeni, A., Masiero, L., Gasparini, P., Zamponi, R., Bartek, J., Lukas, J., and Helin, K. (2004) *J. Cell Biol.* **165,** 473–482
10. Lin, J. J., and Dutta, A. (2007) *J. Biol. Chem.* **282,** 30357–30362
11. McGarry, T. J. (2002) *Mol. Biol. Cell.* **13,** 3662–3671
12. Tachibana, K. E., Gonzalez, M. A., Guarguaglini, G., Nigg, E. A., and Laskey, R. A. (2005) *EMBO Rep.* **6,** 1052–1057
13. Zhu, W., and Depamphilis, M. L. (2009) *Cancer Res.* **69,** 4870–4877
14. Shreeram, S., Sparks, A., Lane, D. P., and Blow, J. J. (2002) *Oncogene* **21,** 6624–6632
15. Kroll, K. L., Salic, A. N., Evans, L. M., and Kirschner, M. W. (1998) *Development* **125,** 3247–3258
16. Del Bene, F., Tessmar-Raible, K., and Wittbrodt, J. (2004) *Nature* **427,** 745–749
17. Luo, L., Yang, X., Takihara, Y., Knoetgen, H., and Kessel, M. (2004) *Nature* **427,** 749–753
18. Seo, S., Herr, A., Lim, J. W., Richardson, G. A., Richardson, H., and Kroll, K. L. (2005) *Genes Dev.* **19,** 1723–1734
19. Papanayotou, C., Mey, A., Birot, A. M., Saka, Y., Boast, S., Smith, J. C., Samarut, J., and Stern, C. D. (2008) *PLoS Biol.* **6,** e2
20. Lee, C., Hong, B., Choi, J. M., Kim, Y., Watanabe, S., Ishimi, Y., Enomoto, T., Tada, S., Kim, Y., and Cho, Y. (2004) *Nature* **430,** 913–917
21. Saxena, S., Yuan, P., Dhar, S. K., Senga, T., Takeda, D., Robinson, H., Kornbluth, S., Swaminathan, K., and Dutta, A. (2004) *Mol. Cell* **15,** 245–258
22. Thépaut, M., Maiorano, D., Guichou, J. F., Augé, M. T., Dumas, C., Méchali, M., and Padilla, A. (2004) *J. Mol. Biol.* **342,** 275–287
23. De Marco, V., Gillespie, P. J., Li, A., Karantzelis, N., Christodoulou, E., Klompmaker, R., van Gerwen, S., Fish, A., Petoukhov, M. V., Iliou, M. S., Lygerou, Z., Medema, R. H., Blow, J. J., Svergun, D. I., Taraviras, S., and Perrakis, A. (2009) *Proc. Natl. Acad. Sci. U.S.A.* **106,** 19807–19812
24. Gemünd, C., Ramu, C., Altenberg-Greulich, B., and Gibson, T. J. (2001) *Nucleic Acids Res.* **29,** 1272–1277
25. Lupas, A., Van Dyke, M., and Stock, J. (1991) *Science* **252,** 1162–1164
26. Puntervoll, P., Linding, R., Gemünd, C., Chabanis-Davidson, S., Mattingsdal, M., Cameron, S., Martin, D. M., Ausiello, G., Brannetti, B., Costantini, A., Ferrè, F., Maselli, V., Via, A., Cesareni, G., Diella, F., Superti-Furga, G., Wyrwicz, L., Ramu, C., McGuigan, C., Gudavalli, R., Letunic, I., Bork, P., Rychlewski, L., Küster, B., Helmer-Citterich, M., Hunter, W. N., Aasland, R., and Gibson, T. J. (2003) *Nucleic Acids Res.* **31,** 3625–3630
27. Larkin, M. A., Blackshields, G., Brown, N. P., Chenna, R., McGettigan, P. A., McWilliam, H., Valentin, F., Wallace, I. M., Wilm, A., Lopez, R., Thompson, J. D., Gibson, T. J., and Higgins, D. G. (2007) *Bioinformatics* **23,** 2947–2948
28. Mooij, W. T., Mitsiki, E., and Perrakis, A. (2009) *Nucleic Acids Res.* **37,** W402–W405
29. Roukos, V., Iliou, M. S., Nishitani, H., Gentzel, M., Wilm, M., Taraviras, S., and Lygerou, Z. (2007) *J. Biol. Chem.* **282,** 9346–9357
30. Ballabeni, A., Melixetian, M., Zamponi, R., Masiero, L., Marinoni, F., and Helin, K. (2004) *EMBO J.* **23,** 3122–3132
31. Xouri, G., Squire, A., Dimaki, M., Geverts, B., Verveer, P. J., Taraviras, S., Nishitani, H., Houtsmuller, A. B., Bastiaens, P. I., and Lygerou, Z. (2007) *EMBO J.* **26,** 1303–1314
32. Xouri, G., Lygerou, Z., Nishitani, H., Pachnis, V., Nurse, P., and Taraviras, S. (2004) *Eur. J. Biochem.* **271,** 3368–3378
33. Spella, M., Britz, O., Kotantaki, P., Lygerou, Z., Nishitani, H., Ramsay, R. G., Flordellis, C., Guillemot, F., Mantamadiotis, T., and Taraviras, S. (2007) *Neuroscience* **147,** 373–387
34. Luna-Vargas, M. P., Christodoulou, E., Alfieri, A., van Dijk, W. J., Stadnik, M., Hibbert, R. G., Sahtoe, D. D., Clerici, M., Marco, V. D., Littler, D., Celie, P. H., Sixma, T. K., and Perrakis, A. (2011) *J. Struct Biol.*, doi:10.1016/j.jsb.2011.03.017
35. Krissinel, E., and Henrick, K. (2007) *J. Mol. Biol.* **372,** 774–797
36. Acquaviva, C., and Pines, J. (2006) *J. Cell Sci.* **119,** 2401–2404
37. Boos, A., Lee, A., Thompson, D. M., and Kroll, K. L. (2006) *Biol. Cell.* **98,** 363–375
38. Hodgson, B., Li, A., Tada, S., and Blow, J. J. (2002) *Curr. Biol.* **12,** 678–683
39. Kroll, K. L. (2007) *Front. Biosci.* **12,** 1395–1409
40. Caro, E., Castellano, M. M., and Gutierrez, C. (2007) *Nature* **447,** 213–217
41. Luo, L., and Kessel, M. (2004) *Cell Cycle* **3,** 711–714
42. Caro, E., and Gutierrez, C. (2007) *Trends Cell Biol.* **17,** 580–585
43. Balestrini, A., Cosentino, C., Errico, A., Garner, E., and Costanzo, V. (2010) *Nat. Cell Biol.* **12,** 484–491
44. Robbins, J., Dilworth, S. M., Laskey, R. A., and Dingwall, C. (1991) *Cell* **64,** 615–623
45. Pfleger, C. M., and Kirschner, M. W. (2000) *Genes Dev.* **14,** 655–665
46. Sugimoto, N., Kitabayashi, I., Osano, S., Tatsumi, Y., Yugawa, T., Narisawa-Saito, M., Matsukage, A., Kiyono, T., and Fujita, M. (2008) *Mol. Biol. Cell.* **19,** 1007–1021
47. Mailand, N., and Diffley, J. F. (2005) *Cell* **122,** 915–926
48. Petersen, B. O., Wagener, C., Marinoni, F., Kramer, E. R., Melixetian, M., Lazzerini Denchi, E., Gieffers, C., Matteucci, C., Peters, J. M., and Helin, K. (2000) *Genes Dev.* **14,** 2330–2343
49. Furuta, Y., Piston, D. W., and Hogan, B. L. (1997) *Development* **124,** 2203–2212
50. Grove, E. A., Tole, S., Limon, J., Yip, L., and Ragsdale, C. W. (1998) *Development* **125,** 2315–2325
51. Monuki, E. S., Porter, F. D., and Walsh, C. A. (2001) *Neuron* **32,** 591–604
52. Shimogori, T., Banuchi, V., Ng, H. Y., Strauss, J. B., and Grove, E. A. (2004) *Development* **131,** 5639–5647